Japanese Journal of
Applied Physics

REGULAR PAPER

Cyclic C_4F_8 and O_2 plasma etching of TiO_2 for high-aspect-ratio three-dimensional devices

To cite this article: Tsubasa Imamura *et al* 2021 *Jpn. J. Appl. Phys.* **60** 036001

Japanese Journal of Applied Physics **60**, 036001 (2021) **REGULAR PAPER**
https://doi.org/**10.35848/1347-4065/abdf78**

Cyclic C_4F_8 and O_2 plasma etching of TiO_2 for high-aspect-ratio three-dimensional devices

Tsubasa Imamura[1,2], Itsuko Sakai[1*], Hisataka Hayashi[1], Makoto Sekine[2], and Masaru Hori[2]

[1]*Process Technology Research & Development Center, Kioxia Corporation, Yokkaichi, Mie 512-8550, Japan*
[2]*Center for Low-temperature Plasma Sciences, Nagoya University, Nagoya 464-8603, Japan*

[*]E-mail: tsubasa.imamura@kioxia.com

Received November 19, 2020; revised January 7, 2021; accepted January 25, 2021; published online February 12, 2021

The present study investigates the cyclic etching of TiO_2 with CF polymer deposition and removal. We find that C_4F_8 plasma treatment forms a CF polymer deposition layer on the TiO_2 and a modified TiO_2 surface under the CF polymer layer. Subsequent O_2 plasma treatment removes the CF polymer and the modified layer at the same time. This sequence is repeated. Accordingly, the TiO_2 film is etched at a rate of 0.67 nm per cycle. The CF polymer and modified TiO_2 layer also form on the sidewall TiO_2 surface of a trench pattern. We realize the isotropic TiO_2 etching of a trench pattern having a high aspect ratio exceeding 40 adopting the cyclic C_4F_8 and O_2 plasma process. © 2021 The Japan Society of Applied Physics

1. Introduction

Flash memory devices have changed from planar to three-dimensional (3D) structures, comprising vertically stacked memory cells that require the formation of small and high-aspect-ratio spaces, to meet market demands for increased storage capacity. In general, 3D flash memory has a plurality of holes formed by alternating layers of conducting and insulating materials. The conducting layers act as control gates. Memory cells form on the sidewalls of holes. A memory cell usually comprises a SiO_2 layer, Si_3N_4 layer, and another SiO_2 layer as a gate dielectric, a charge trap layer, and a tunnel dielectric layer. These memory cell layers do not require insulation between control gates. However, some types of 3D memory require the insulation of memory cells. Such types of 3D memory require the recession of conducting materials after holes are formed for this purpose. Memory cell films are then deposited along the recessed regions and the sidewalls, and predetermined portions of the films are removed to provide insulation through isotropic etching.[1–4] A challenging requirement of 3D memory devices is to control the amount of etching of these films precisely. Moreover, the most difficult aspect of this process is that the amount of etching needs to be uniform from the top to the bottom of the high-aspect-ratio pattern. The memory cell films comprise various materials, such as W, TiN, Al_2O_3, HfO_2, ZrO_2, TiO_2, Si, Si_3N_4, and SiO_2.[5]

Several studies have investigated isotropic atomic layer etching (ALE) to meet the demand for increased storage capacity in recent years.[6–25] These studies can be classified as those on wet ALE and those on thermal ALE. Yin et al. demonstrated isotropic SiGe etching adopting wet solution oxidation.[7] However, the wet process faces the problem of pattern collapse.[8] Thermal ALE, called ligand exchange,[9–13] and conversion etching[14–17] have been employed for metal oxide materials; e.g. Al_2O_3, HfO_2, ZrO_2, ZnO, WO_3, TiO_2, GaN, and SiO_2. These processes are the reverse of atomic layer deposition, which requires a high temperature exceeding 150 °C and a metal coreagent such as trimethylaluminum, tin acetylacetone, dimethylaluminum chloride, or silicon tetrachloride. Izawa's group reported the thermal ALE of Si_3N_4 using the formation and desorption of ammonium fluorosilicate.[18–20] They used fluorocarbon radicals to form ammonium fluorosilicate on a Si_3N_4 surface at room temperature and then desorbed the ammonium fluorosilicate at a temperature exceeding 100 °C. This requires a cycle of wafer cooling and annealing, and they thus developed a special 300 mm tool with an infrared lamp for rapid cycling.[19] In addition, the high-temperature process adopted in thermal ALE can degrade the device performance. A low-temperature process that can be realized preferentially with a conventional tool is thus needed.

In this paper, we report on an isotropic cycle etching of TiO_2 that can be realized at a low temperature of 60 °C using a conventional capacitively coupled plasma (CCP) reactive ion etching (RIE) tool. We suggest the mechanism of cycle etching and demonstrate the sidewall TiO_2 etching of a trench pattern with a high aspect ratio of more than 40.

2. Experimental methods

A 10 nm thick amorphous TiO_2 blanket film was deposited on a 300 mm Si wafer through atomic layer deposition. We used tetrakis dimethyl amino titanium and O_3 as a precursor and oxidant, respectively. The process temperature of the atomic layer deposition was 200 °C. In addition to the blanket sample, we used two types of patterned sample having different aspect ratios. One was a SiO_2 line and space pattern with an aspect ratio 16.5. The 330 nm thick SiO_2 was deposited on 30 nm thick Si_3N_4 and etched through RIE. We used spin-on-coat polymer film as the SiO_2 etching mask of the line and space pattern with a half-pitch of 40 nm. After the SiO_2 etching, the spin-on-coat film was removed through ashing. A 10 nm thick layer of TiO_2 was then deposited. The space after TiO_2 deposition was 20 nm. The other sample was a SiO_2 trench pattern with an aspect ratio of 46. The 3500 nm thick SiO_2 was deposited on a Si substrate and etched through RIE. We used amorphous carbon film with a slit width of 100 nm as the mask of the trench pattern. The carbon layer was removed after SiO_2 RIE. A 10 nm thick layer of TiO_2 was deposited and the space after the deposition was 80 nm. Etching experiments were carried out using a CCP RIE system (Tokyo Electron, Vesta-RBH). Radio-frequency (100 MHz) power was applied to the substrate to induce plasma. Conditions to which the TiO_2 film was exposed are listed in Table I. Ellipsometry was adopted to measure the thickness of the TiO_2 blanket film and the etched amount of film was calculated from the thickness before and after the plasma treatments. Transmission electron

Table I. Plasma exposure conditions of TiO_2 samples.

	CF_4 plasma	C_4F_8 plasma	O_2 plasma
Pressure (Pa)	1.3	1.3	13.3
Gas	CF_4	C_4F_8	O_2
Gas flow rate (sccm)	100	100	300
100 MHz RF power (W)	1000	1000	1000
Stage temperature (°C)	60	60	60

microscopy (TEM) was adopted to measure the sidewall TiO_2 film thickness of the pattern samples. We also adopted X-ray photoelectron spectroscopy (XPS) to investigate the bonding states of the blanket film surface and energy dispersive X-ray spectroscopy (EDX) to analyze the atomic composition of the sidewall film of the pattern samples.

3. Results and discussion

3.1. TiO_2 etching with CF_4 plasma

Figure 1 shows the amount of etching of the TiO_2 blanket film with CF_4 plasma. The plasma conditions were pressure of 1.3 Pa, 100 MHz radio-frequency power of 1000 W, a CF_4 gas flow rate of 100 sccm, and a substrate temperature of 60 °C. The etched amount increased linearly with the treatment time as expected and the etching rate was 12.5 nm min^{-1}. We next confirm the amount of etching of the sidewall TiO_2 film. Figure 2(a) shows the cross-sectional TEM image of the line and space patterned sample with an aspect ratio of 16.5. Figure 2(b) shows the cross-sectional TEM image after CF_4 plasma treatment for 30 s. The depth dependence of the sidewall TiO_2 film thickness before and after the CF_4 plasma treatment and the etched amount are plotted in Fig. 3. The depth is defined as being from the top of the pristine pattern. The deposited TiO_2 film thickness varies from 10.1 nm at a depth of 40 nm to 9.8 nm at a depth of 300 nm. The remaining TiO_2 film thickness after the plasma treatment increased from 7.5 nm at 40 nm to 8.3 nm at 300 nm. The etched amount therefore decreased from 2.6 nm at 40 nm to 1.5 nm at 300 nm. Woo et al. showed the mechanism of the etching of TiO_2 film with CF_4 plasma.[26] They mentioned that the TiO_2 film reacted with F radicals from the CF_4 plasma because the Ti–F chemical bond is stronger than the Ti–O bond, and TiF_x formed on the surface as a byproduct. The TiF_x was removed by ion bombardment. We believe that the amount of F radical decreased from the top of the pattern to the bottom because the radicals having diffused from the plasma were consumed on the sidewall. This caused the dependence of the etched amount on the pattern depth, or aspect ratio. Therefore, to suppress this dependence, we considered it important to supply the same amount of F radicals regardless of the aspect ratio, and one method would be to use the CF polymer formed on the TiO_2 surface. We supposed the same amount of F radical could be provided from the CF polymer from top to bottom of the hole when etching with O_2 plasma. In this study, we used C_4F_8 plasma to form the CF polymer.

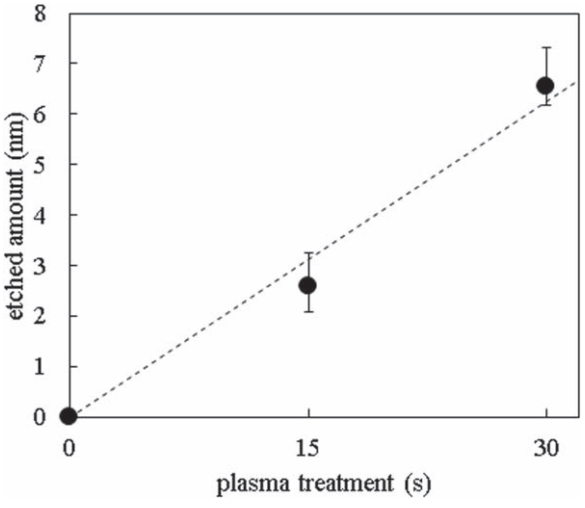

Fig. 1. Etched amount of the blanket TiO_2 as a function of the CF_4 plasma treatment time (30 and 60 s).

3.2. Blanket TiO_2 etching with cyclic C_4F_8 and O_2 plasma

First, blanket TiO_2 etching was carried out with cyclic C_4F_8 and O_2 plasma processing. Figure 4 shows the cyclic number dependence of blanket TiO_2 etching with cyclic C_4F_8 and O_2 plasma. Both treatment times were 30 s. The etched amount increased linearly with the number of cycles. The TiO_2 etched amount per cycle was 0.71 nm/cycle. We also confirmed the O_2 plasma did not etch the TiO_2 film. This result supports that F radicals from the CF polymer etched TiO_2. We next confirm the dependence of the TiO_2 etched amount on the CF polymer thickness. We first measured CF polymer thicknesses for different C_4F_8 plasma treatment times from cross-sectional SEM images. Figure 5 shows that the thickness increased linearly with the treatment time. We then measured the TiO_2 etched amounts for the different CF polymer thicknesses. The TiO_2 etched amounts were 0.74 and 0.80 nm when the CF polymer thicknesses were 13.6 and 27.6 nm, respectively. The O_2 plasma treatment time was 30 s and there was one cycle. These results indicate that the TiO_2 etched amount was constant even if the thickness of the CF polymer formed on the film surface was different. We next analyze cross-sectional images after taken each step to investigate whether TiO_2 etching is constant regardless of the CF polymer thickness.

Figure 6 shows TEM images as the TiO_2 was deposited [Fig. 6(a)], after C_4F_8 plasma treatment [Fig. 6(b)], and after O_2 plasma treatment [Fig. 6(c)]. Both plasma treatment times were 30 s. The TiO_2 thickness increased from 10.1 nm as TiO_2 was deposited to 10.5 nm after C_4F_8 plasma treatment, and then decreased to 9.4 nm after O_2 plasma treatment. This means that TiO_2 was not etched by C_4F_8 plasma but etched by O_2 plasma. The sample after C_4F_8 plasma treatment [Fig. 6(b)] shows that there was a modified layer between the CF polymer and TiO_2 surface. The modified layer was removed with O_2 plasma treatment [Fig. 6(c)]. Figure 7 shows the TEM images after C_4F_8 plasma treatment for 30 s [Fig. 7(a)] and 60 s [Fig. 7(b)]. The thickness of the modified layer after 60 s was the same as that after 30 s although the CF polymer after 60 s was thicker than that after 30 s. This shows that the modified layer thickness is constant regardless of the CF polymer thickness. We speculate that the TiO_2 surface is modified by CF radicals with ion bombardment and not with thermal energy from the stage. However, the thick CF polymer protects the surface from ions. Therefore, the modified layer is kept constant, although the CF polymer thickness increases. As a result, the TiO_2 etched amount is constant even if the CF polymer thickness changes. We then

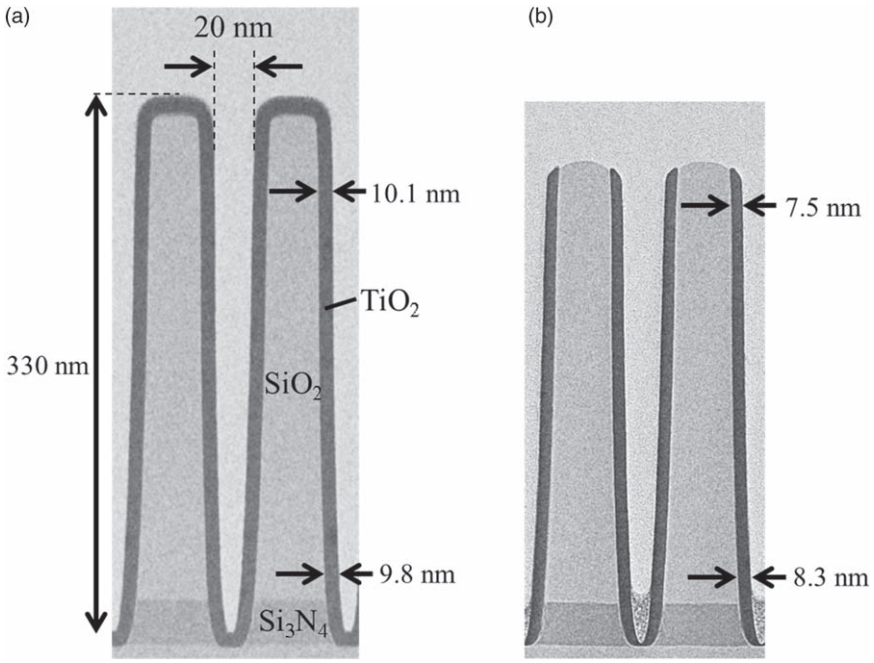

Fig. 2. Cross-sectional TEM images: (a) as deposited and (b) after CF_4 plasma treatment for 30 s.

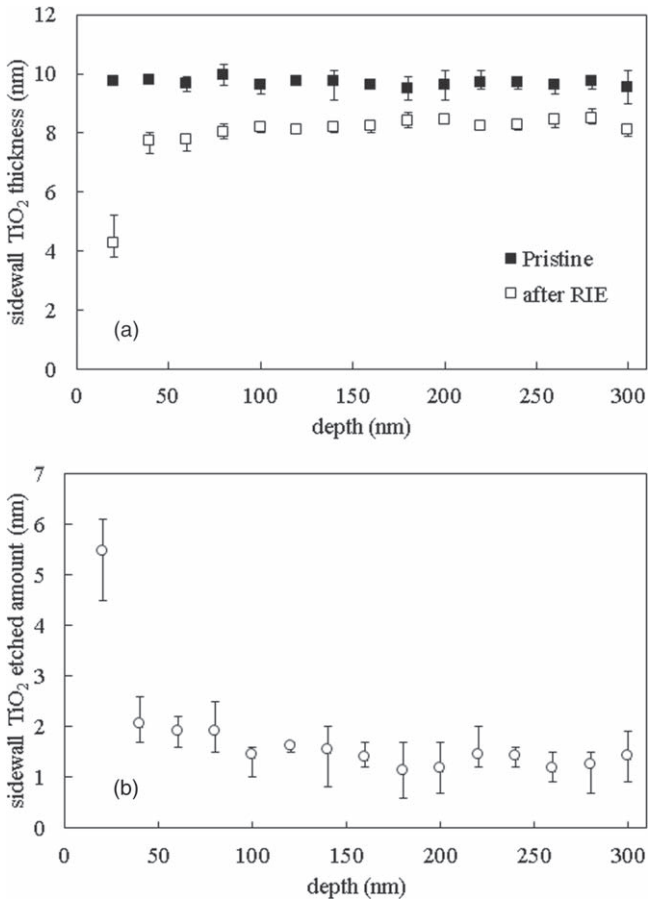

Fig. 3. (a) Depth dependence of the sidewall TiO_2 thicknesses before and after CF_4 plasma treatment for 30 s and (b) the sidewall etched amount.

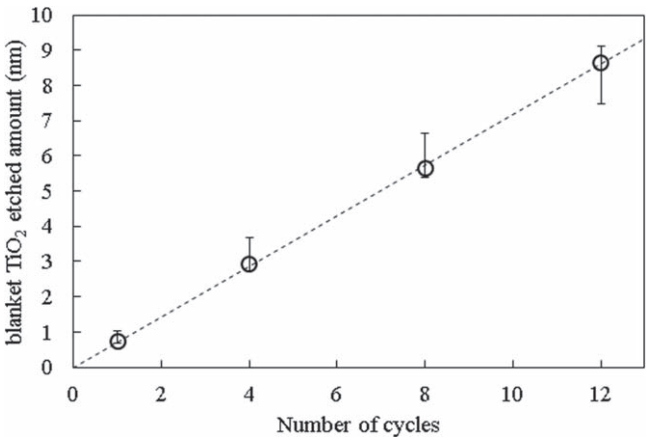

Fig. 4. Cyclic number dependence of the amount of blanket TiO_2 etching with cyclic C_4F_8 and O_2 plasma.

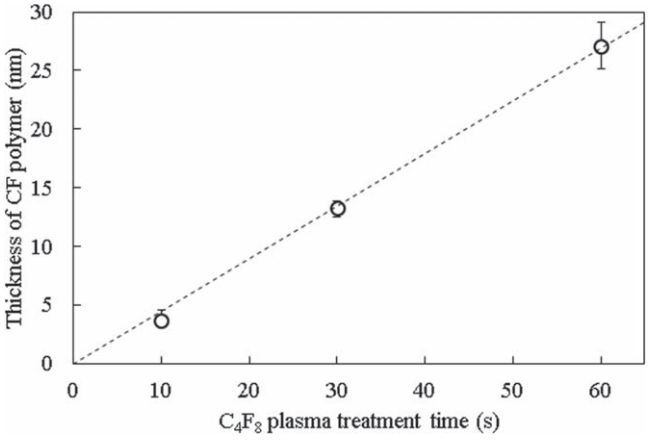

Fig. 5. CF polymer thickness on the blanket TiO_2 film for different C_4F_8 plasma treatment times.

carried out XPS analysis to investigate the TiO_2 surface after removal of the modified layer.

Figure 8 shows the narrow-scan spectra of (a) Ti, (b) F, and (c) C of both the pristine sample and sample after C_4F_8 plasma and O_2 plasma treatment. The sample after these plasma treatments had a single peak at around 684 eV related to F 1s, while the pristine sample did not [Fig. 8(b)]. This means that there was F residue on the surface after the plasma treatments. Figure 8(c) shows the spectrum of C 1s. Both samples had two peaks at 284.8 and 288.9 eV, which

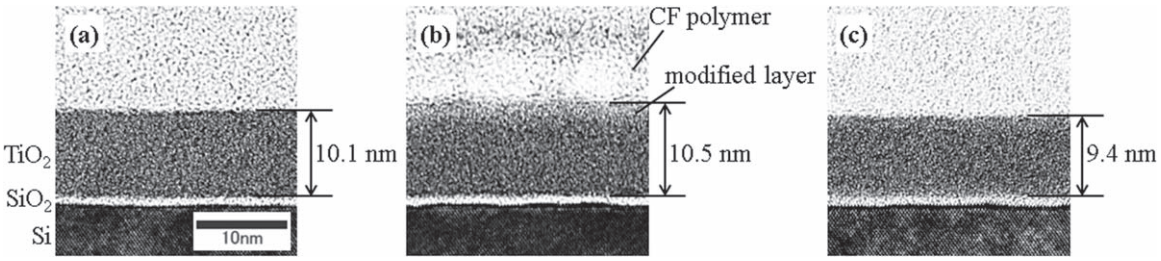

Fig. 6. TEM images: (a) as TiO_2 deposited, (b) after C_4F_8 plasma treatment, and (c) after O_2 plasma treatment.

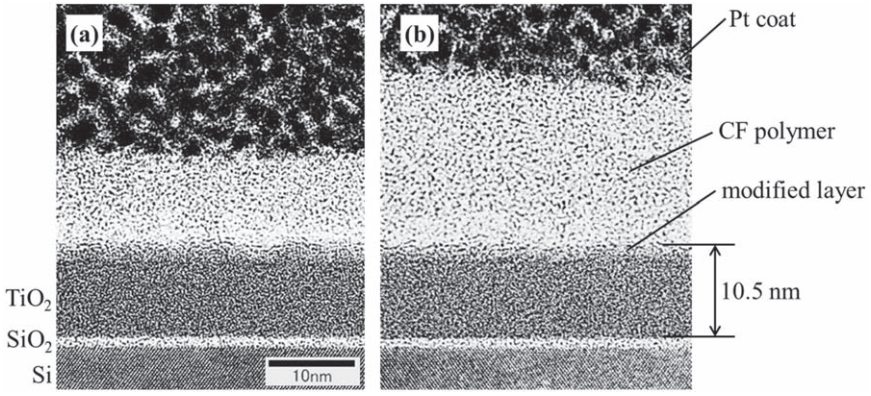

Fig. 7. TEM images of TiO_2 film after C_4F_8 plasma treatment for (a) 30 s and (b) 60 s.

correspond to C–C and O–C=O bonds, respectively. These peaks are considered to be due to surface impurities. This result supports the finding that the F residue after the plasma treatments was not CF polymer. The spectrum of Ti 2p in the pristine sample had two peaks at 458.8 and 464.6 eV owing to the titanium atoms of TiO_2 [Fig. 8(a)], and the spectrum after the plasma treatments had two peaks at 459.1 and 464.9 eV. These peaks were also due to TiO_2 but they were slightly shifted to higher energy, which indicates Ti–F bonds on the surface.[26] The surface after the plasma treatments thus contained TiO_2 and TiF_x. We speculate that the TiF_x is the residue of the modified layer. We finally conducted thermal desorption spectroscopy after each step to investigate the detail of the modified layer.

Figure 9 shows ion currents for mass-to-charge ratios of 67, 86, 105, and 124, which respectively correspond to TiF, TiF_2, TiF_3, and TiF_4. The spectroscopies of TiF and TiF_3 had two peaks at 350 °C and 460 °C while TiF_2 and TiF_4 had a single peak at 350 °C. We believe that there were two types of titanium fluoride. One had a desorption peak at 350 °C and dissociated into TiF, TiF_2, TiF_3, and TiF_4 in the mass spectrometer. The other had a peak at 450 °C and dissociated into TiF and TiF_3 [Fig. 9(a)]. There were no peaks of these except for TiF in the sample after the O_2 plasma treatment [Fig. 9(b)]. The TiF peak count was 1.78×10^{-13} A having decreased from 1.00×10^{-12} A after the C_4F_8 plasma treatment. These results show that the modified layer that formed in the C_4F_8 plasma was titanium fluorides and most of it was etched away with O_2 plasma. We finally confirm that the etched amount depends on the stage temperatures in the C_4F_8 plasma step and O_2 plasma step.

Figure 10 shows the blanket TiO_2 etched amount for different stage temperatures in each step. We first decreased the temperature of the C_4F_8 plasma step from 60 °C to 20 °C, while the O_2 plasma step had a temperature of 60 °C. The etched amount per cycle in the C_4F_8 plasma step at 20 °C was 0.63 nm/cycle, which was almost same as that at 60 °C. We then decreased the temperature in the O_2 plasma step from 60 °C to 20 °C, while the C_4F_8 plasma step had a temperature of 60 °C. The etched amount per cycle in the O_2 plasma step at 20 °C was 0.24 nm/cycle, which was lower than that at 60 °C. These results show that the thickness of the modified layer formed in the C_4F_8 plasma step does not depend on the temperature, while the etched amount of the modified layer in the O_2 plasma step does. This is consistent with the results of thermal desorption spectroscopy. However, the calculated vapor pressure of TiF_4 at 60 °C was 0.14 Pa,[27] which was lower than the pressure of the O_2 plasma of 13.3 Pa by a factor of 95. We therefore believe that the etching reaction is assisted by ion bombardment in the O_2 plasma treatment.

On the basis of the above results, we suggest the TiO_2 etching mechanism of the cyclic process shown in Fig. 11. First, the C_4F_8 plasma modifies the surface of the TiO_2 and formed TiF, TiF_2, TiF_3, and TiF_4 [Fig. 11(a)]. The titanium fluorides remain on the surface because their vapor pressure is lower than the plasma pressure. The CF polymer therefore forms on the titanium fluorides [Fig. 11(b)]. Consequently, the CF polymer suppresses further modification and formation of titanium fluorides. O radicals and ions in the O_2 plasma remove the CF polymer and TiF_2, TiF_3, and TiF_4 [Figs. 11(c), 11(d)]. TiF remains on the surface and changes to TiF_x in the next C_4F_8 plasma step.

3.3. Cyclic C_4F_8 and O_2 plasma etching of sidewall TiO_2

This section reports on the application of the cyclic process to a sidewall TiO_2 film on a line pattern.

First, we measured the profile of the film composition to study the surface state of the sidewall TiO_2 film after the C_4F_8 plasma treatment. Figure 12(a) shows the TEM image of the pattern sample after C_4F_8 plasma treatment for 30 s.

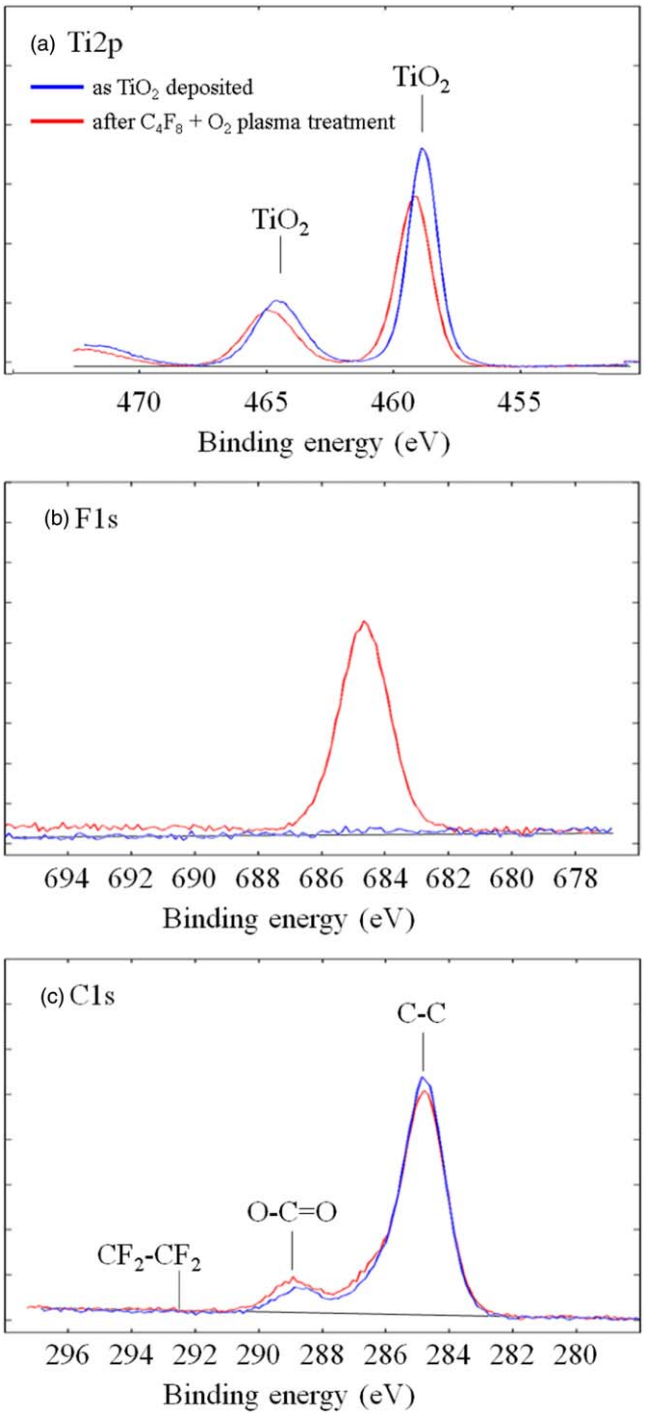

Fig. 8. (Color online) Narrow-scan XPS spectra of the blanket TiO_2 surface and the film after C_4F_8 plasma and O_2 plasma treatment: (a) Ti 2p, (b) F 1s, and (c) C 1s.

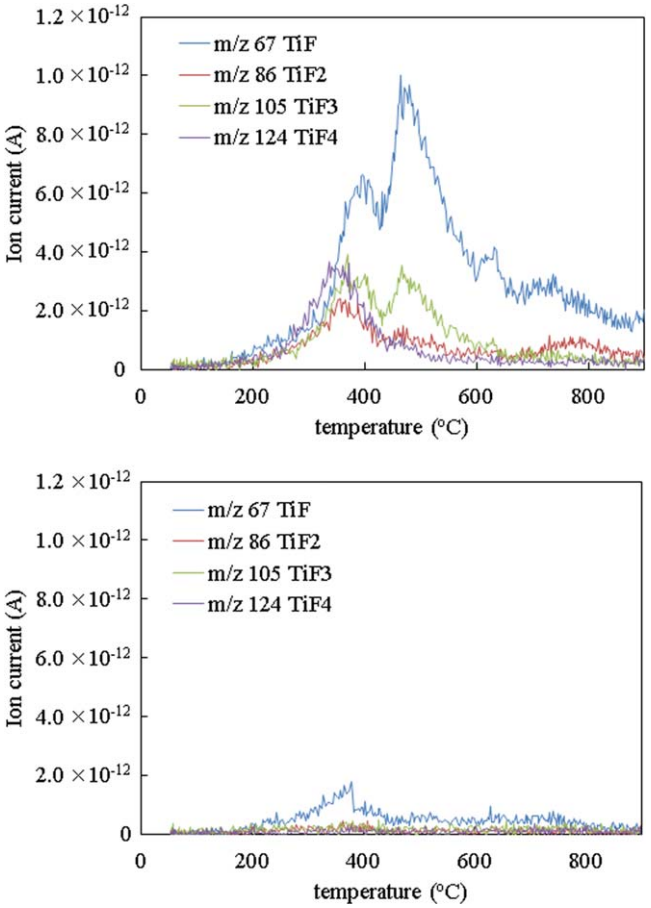

Fig. 9. (Color online) Ion currents of thermal desorption spectroscopy (a) after C_4F_8 plasma treatment and (b) after O_2 plasma treatment. Mass-to-charge ratios of 67, 86, 105, and 124 correspond to TiF, TiF_2, TiF_3, and TiF_4, respectively.

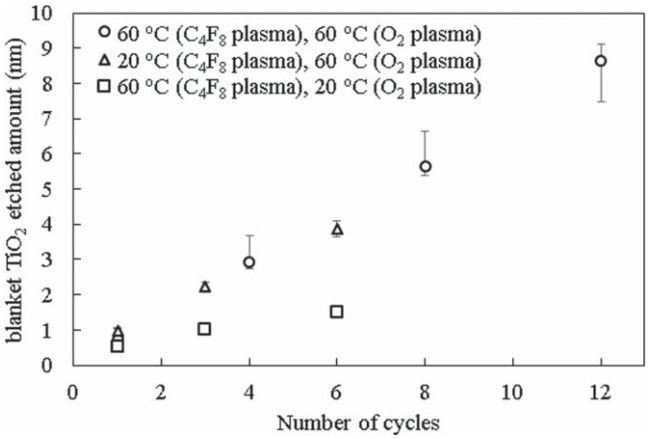

Fig. 10. Cyclic number dependence of the blanket TiO_2 etched amount at different stage temperatures; (○) both steps had temperatures of 60 °C, (△) the C_4F_8 plasma had a temperature of 20 °C and the O_2 plasma a temperature of 60 °C, (□) and the C_4F_8 plasma had a temperature of 60 °C and the O_2 plasma a temperature of 20 °C. The plasma treatment time was 30 s under all conditions.

Figures 12(b) and 12(c) shows the atomic percentages of C, F, Ti, and Si, which were obtained by EDX spectroscopy, at the upper and lower portions shown in Fig. 12(a), respectively. The horizontal axis shows the distance from the line pattern while the vertical axis shows the atomic percentage. The Ti increases from below 1% at 2 nm to above 20% at 8 nm as the Si decreases from above 25% to below 1% in both Figs. 12(b) and 12(c). We believe that the boundary between the SiO_2 and TiO_2 film was at about 5 nm. Meanwhile, the boundary between the TiO_2 film and CF polymer is unclear in both the upper portion [Fig. 12(b)] and lower portion [Fig. 12(c)]. In both portions, Ti decreased from above 20% at 20 nm to below 1% at 25 nm, C increased from below 3% at 15 nm to above 80% at 24 nm, and F was above 3% in the range from 14 to 22 nm. Therefore, there were Ti, C, and F in the range from 15 to 20 nm. This means that TiO_2 film and CF polymer were mixed at the boundary

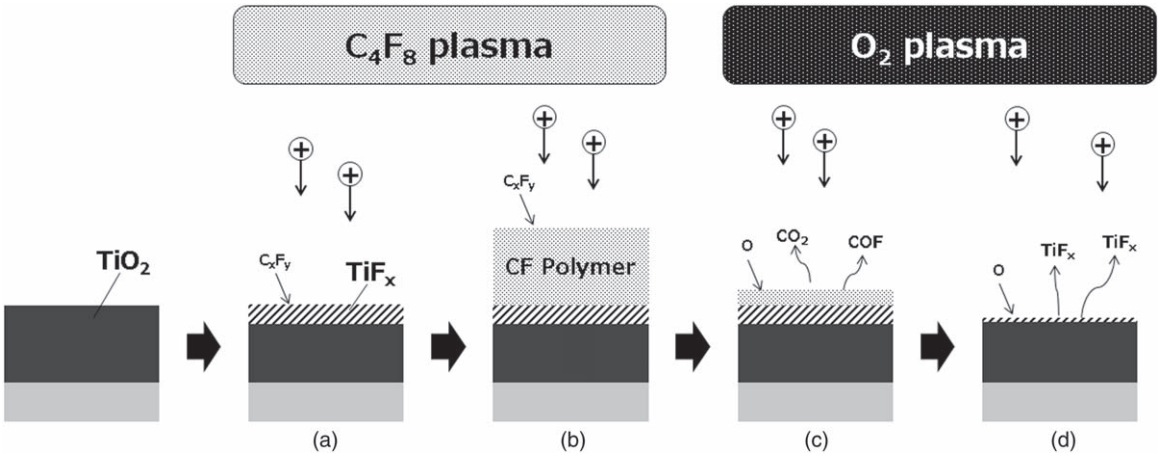

Fig. 11. Schematic flow of the cyclic C_4F_8 and O_2 plasma etching mechanism. (a) The C_4F_8 plasma modified the surface of the TiO_2. (b) CF polymer formed on the modified surface. O_2 plasma etched (c) the CF polymer and then (d) the modified layer.

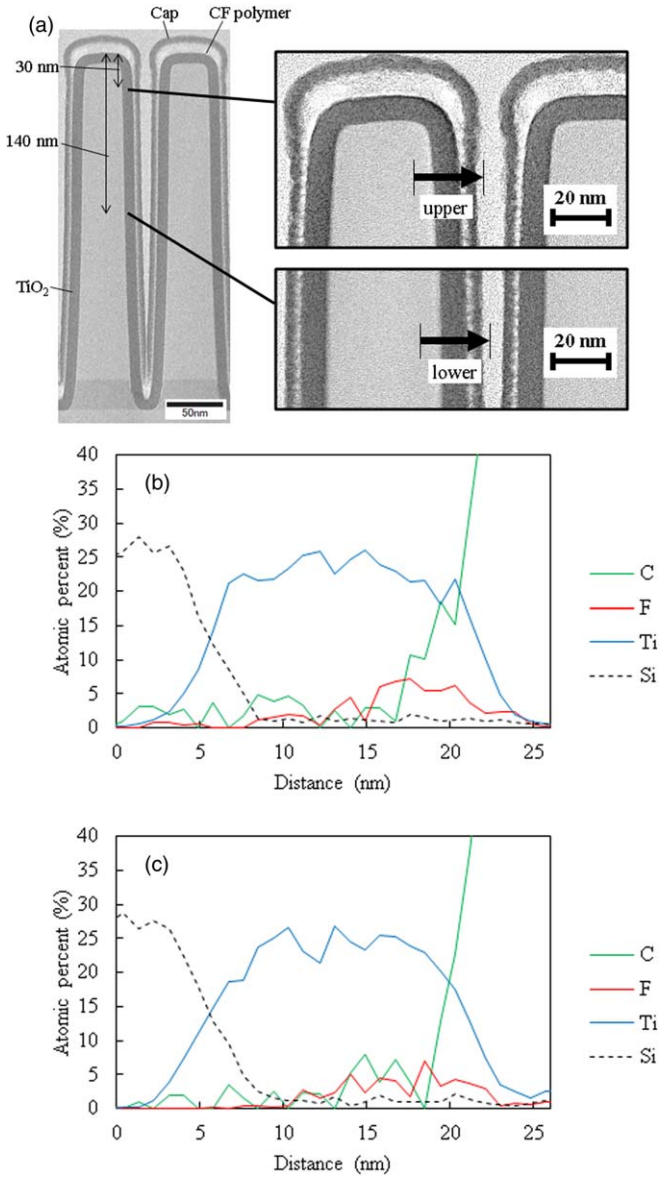

Fig. 12. (Color online) (a) TEM image of the pattern sample after the C_4F_8 plasma treatment for 30 s. The atomic percentages of C, F, Ti, and Si obtained by EDX spectroscopy in (b) the upper portion and (c) the lower portion.

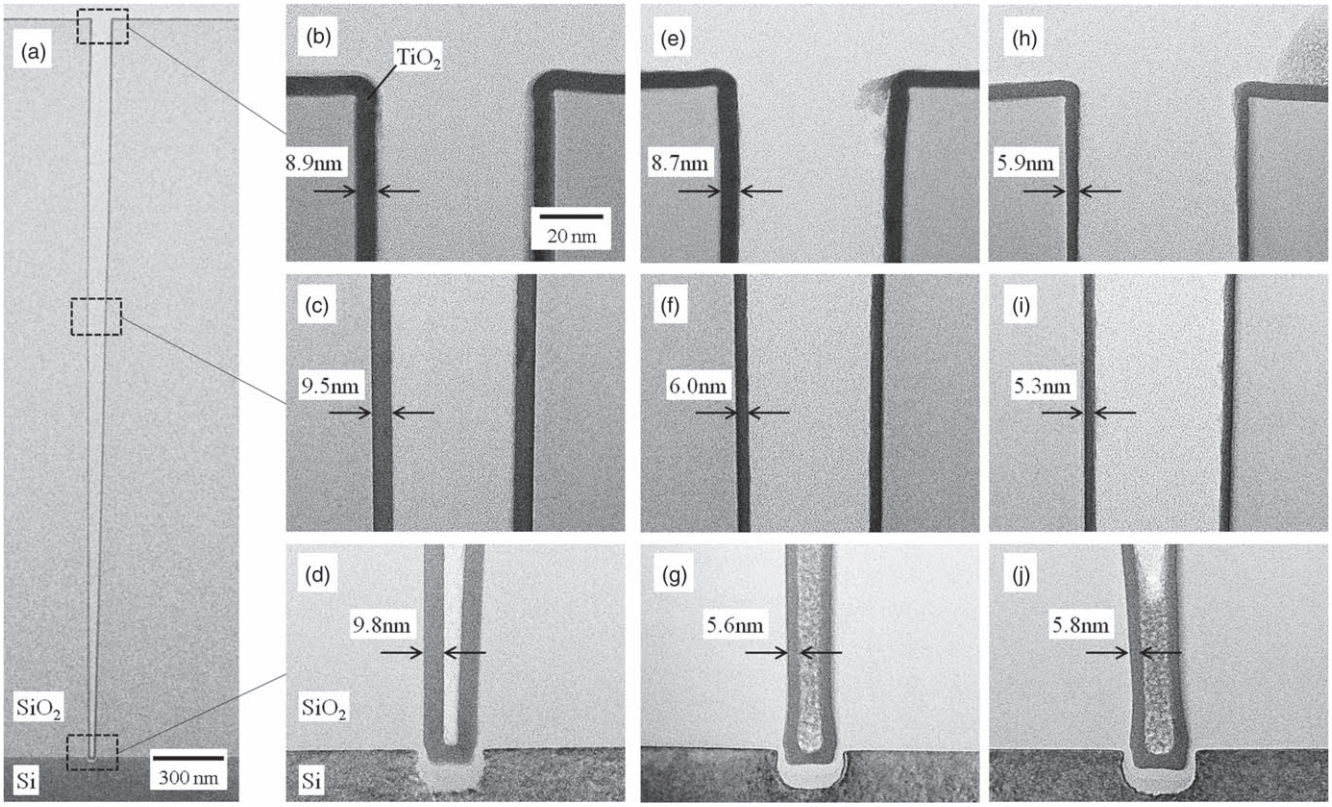

Fig. 13. TEM images of the trench pattern sample as TiO_2 was deposited: (a) perspective of the pattern, (b) enlargement of the top of the pattern, (c) middle of the pattern at a depth of 1400 nm from the top, and (d) the bottom of the pattern. Images (e)–(j) are TEM images after eight cycles of the process. Images show samples after the cyclic process with O_2 plasma treatment for 30 s [(e)–(g)] and 60 s [(h)– (j)].

regardless of the depth. We believe from these results that the sidewall surface was modified by C_4F_8 plasma treatment, the same as for the blanket surface.

Second, we etched the sidewall TiO_2 film on a trench pattern with an aspect ratio of 46. Figure 13(a) shows the TEM image of the trench pattern sample as TiO_2 was deposited. Figures 13(b)–13(d) shows enlargements of Fig. 13(a) at the top, a 1400 nm depth from the top, and the bottom, respectively. We used two O_2 plasma treatment times in the cyclic process. One was 30 s and the other was 60 s. The C_4F_8 plasma treatment time and the number of cycles were held constant at 30 s and eight cycles, respectively. TEM images after the cyclic process with O_2 plasma for 30 s are shown in Figs. 13(e)–13(g) while those for 60 s are shown in Figs. 13(h)–13(j). Figure 14 shows the thickness of sidewall TiO_2 as deposited and after the cyclic processes. The etched amounts were 0.2, 3.4, 3.5, 3.5, 3.1, and 4.2 nm at the top of the pattern, a depth of 700 nm from the top, a depth of 1400 nm, a depth of 2100 nm, a depth of 2800 nm, and the bottom, respectively. The sidewall TiO_2 at the top was not etched and the average etched amount except at the top was 3.5 nm. The amount increased with an increase in the O_2 plasma treatment time from 30 to 60 s. The etched amounts after 60 s were 2.9, 4.3, 4.2, 5.1, 4.3, and 4.0 nm, respectively; i.e. the top sidewall TiO_2 was etched by 2.9 nm and the average etched amount except at the top was 4.4 nm. We believe that O_2 plasma treatment for insufficient time cannot remove the CF polymer completely. The remaining CF polymer then prevents the modified TiO_2 from being removed. Consequently, the etched amount increases with the O_2 plasma treatment time. Furthermore, the CF polymer

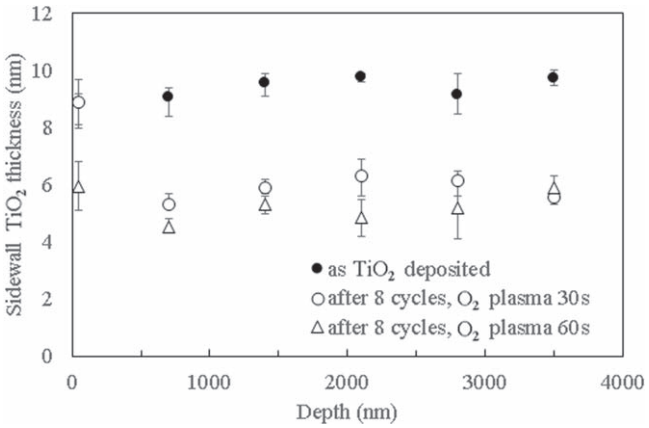

Fig. 14. Sidewall TiO_2 thicknesses of the trench pattern samples as deposited and after the cyclic processes.

thickness at the top is greater than that of the sidewall in the trench as shown in Fig. 12(a), which results in a smaller amount of etching at the top.

4. Conclusions

Cycle etching of TiO_2 was performed using C_4F_8 and O_2 plasma. We confirmed that C_4F_8 plasma formed a CF polymer layer on TiO_2 and a modified TiO_2 layer under the CF polymer, and most of the modified layer was removed by the following O_2 plasma treatment. We believe that the modified layer comprises several types of titanium fluoride, and they do not desorb from the surface in the C_4F_8 plasma step because of their low vapor pressure and the CF polymer formed on the modified layer. In addition, the desorption

amount of the modified layer in the O_2 plasma step depends on the temperature, and we can thus control the etched amount per cycle using the temperature of the step. The cyclic process of these two steps successfully etched TiO_2 and the etching amount increased in proportion to the number of cycles. The etch rate was 0.67 nm/cycle. We also confirmed uniform sidewall etching of TiO_2 film formed on a trench patterned sample with an aspect ratio of 46. We believe that the C_4F_8 and O_2 plasma cyclic process is a promising way to etch a sidewall uniformly in future-generation 3D devices.

1) F. A. Simsek-Ege and N. Ramaswamy, U.S. Patent 10141322 (2018).
2) S.-C. Lai, U.S. Patent 9356040 (2016).
3) J. Alsmeier, U.S. Patent 8445347 (2013).
4) M. Fujiwara et al., Proc. 2019 IEEE Int. Electron Device Meeting (IEDM 2019), 2019, p. 28.1.1.
5) G. D. Wilk, R. M. Wallace, and J. M. Anthony, J. Appl. Phys. **89**, 5243 (2001).
6) C. Fang, Y. Cao, D. Wu, and A. Li, Prog. Nat. Sci.: Mater. Int. **28**, 667 (2018).
7) X. Yin, H. Zhu, L. Zhao, G. Wang, C. Li, W. Huang, Y. Zhang, K. Jia, J. Li, and H. H. Radamson, ECS J. Solid State Sci. Technol. **9**, 034012 (2020).
8) H. Namatsu, K. Kurihara, M. Nagase, K. Iwadate, and K. Murase, Appl. Phys. Lett. **66**, 2655 (1995).
9) Y. Lee and S. M. George, ACS Nano **9**, 2061 (2015).
10) Y. Lee, C. Huffman, and S. M. George, Chem. Mater. **28**, 7657 (2016).
11) Y. Lee, J. W. DuMont, and S. M. George, Chem. Mater. **28**, 2994 (2016).
12) N. R. Johnson, J. K. Hite, M. A. Mastro, C. R. Eddy Jr, and S. M. George, Appl. Phys. Lett. **114**, 243103 (2019).
13) K. J. Kanarik, T. Lill, E. A. Hudson, S. Sriraman, S. Tan, J. Marks, V. Vahedi, and R. A. Gottscho, J. Vac. Sci. Technol. **A33**, 020802 (2015).
14) J. W. DuMont, A. E. Marquardt, A. M. Cano, and S. M. George, ACS Appl. Mater. Interfaces **9**, 10296 (2017).
15) D. R. Zywotko and S. M. George, Chem. Mater. **29**, 1183 (2017).
16) N. R. Johnson and S. M. George, ACS Appl. Mater. Interfaces **9**, 34435 (2017).
17) P. C. Lemaire and G. N. Parsons, Chem. Mater. **29**, 6653 (2017).
18) K. Shinoda, M. Izawa, T. Kanekiyo, K. Ishikawa, and M. Hori, Appl. Phys. Express **9**, 106201 (2016).
19) K. Shinoda, N. Miyoshi, H. Kobayashi, M. Izawa, T. Saeki, K. Ishikawa, and M. Hori, J. Vac. Sci. Technol. **A37**, 051002 (2019).
20) N. Miyoshi, H. Kobayashi, K. Shinoda, M. Kurihara, T. Watanabe, Y. Kouzuma, K. Yokogawa, S. Sakai, and M. Izawa, Jpn. J. Appl. Phys. **56**, 06HB01 (2017).
21) S. Imai, T. Haga, O. Matsuzaki, T. Hattori, and M. Matsumura, Jpn. J. Appl. Phys. **34**, 5049 (1995).
22) H. Nishino, N. Hayasaka, and H. Okano, J. Appl. Phys. **74**, 1345 (1993).
23) J. B. Park, W. S. Lim, S. D. Park, B. J. Park, and G. Y. Yeom, J. Korean Phys. Soc. **54**, 976 (2009).
24) D. Metzler, R. L. Bruce, S. Engelmann, E. A. Joseph, and G. S. Oehrlein, J. Vac. Sci. Technol. A **32**, 020603 (2014).
25) T. Tsutsumi, H. Kondo, M. Hori, M. Zaitsu, A. Kobayashi, T. Nozawa, and N. Kobayashi, J. Vac. Sci. Technol. A **35**, 01A103 (2017).
26) J.-C. Woo, Y.-H. Joo, and C.-I. Kim, Jpn. J. Appl. Phys. **50**, 08KC02 (2011).
27) E. H. Hall, J. M. Blocher, and I. E. Campbell, J. Electrochem. Soc. **105**, 275 (1958).